# Multi-dimensional Simulations of Core-Collapse Supernova Explosions with CHIMERA

O. E. B. Messer[1,2,3,a)], J. A. Harris[1], W. R. Hix[2,3], E. J. Lentz[3], S. W. Bruenn[4] and A. Mezzacappa[3,5]

[1]*Oak Ridge Leadership Computing Facility, Oak Ridge National Laboratory, Oak Ridge, TN 37831 USA*
[2]*Physics Division, Oak Ridge National Laboratory, Oak Ridge, TN 37831 USA*
[3]*Department of Physics & Astronomy, University of Tennessee, Knoxville, TN 37996 USA*
[4]*Department of Physics, Florida Atlantic University, Boca Raton, FL 33431 USA*
[5]*Joint Institute for Computational Sciences, Oak Ridge National Laboratory, Oak Ridge, TN 37831 USA*

[a)]Corresponding author: bronson@ornl.gov

**Abstract.** Unraveling the core-collapse supernova (CCSN) mechanism is a problem that remains essentially unsolved despite more than four decades of effort. Spherically symmetric models with otherwise high physical fidelity generally fail to produce explosions, and it is widely accepted that CCSNe are inherently multi-dimensional. Progress in realistic modeling has occurred recently through the availability of petascale platforms and the increasing sophistication of supernova codes. We will discuss our most recent work on understanding neutrino-driven CCSN explosions employing multi-dimensional neutrino-radiation hydrodynamics simulations with the CHIMERA code. We discuss the inputs and resulting outputs from these simulations, the role of neutrino radiation transport, and the importance of multi-dimensional fluid flows in shaping the explosions. We also highlight the production of $^{48}$Ca in long-running CHIMERA simulations.

## INTRODUCTION

After several million years of evolution and nuclear energy release, a massive star's core is composed of iron (and similar 'iron-peak' elements) from which no further nuclear energy can be released by fission or fusion. Outside the Fe-core are shells representative of previous burning stages— a silicon shell, oxygen shell, etc., out to a helium shell surrounded by an envelope of hydrogen. At the base of the Si-shell, nuclear burning continues, growing the Fe-core below. When the mass of the Fe-core reaches the limiting Chandrasekhar mass, it starts to collapse. For slightly less massive stars ($M$~8–10 $M_\odot$), a similar collapse occurs, but with a core of oxygen and neon.

During the collapse, the inner core will become opaque to neutrinos and surpass the density of atomic nuclei ($\gtrsim 2.5 \times 10^{14}$ g cm$^{-3}$) reaching densities where individual nuclei merge together into nuclear matter. Above nuclear density, the nuclear equation of state (EoS) stiffens and the core rebounds like an over-compressed spring, launching a bounce shock from the newly formed neutron star (a proto-NS; PNS). The shock, initially enclosing ~0.5 $M_\odot$ of the ~1.5 $M_\odot$ Fe-core at a radius of ~10 km, progresses outward through the rest of the infalling core, heating and dissociating the infalling nuclei to free nucleons and radiating a large burst of neutrinos. Thermal energy removed from the shocked material by neutrinos and nuclear dissociation halts the progress of the shock rendering it a standing accretion shock with a radius of 100–200 km about 50 ms after it is launched. In this accreting state, the inner regions of the star continue to collapse and pass through the shock. The shocked, still infalling matter is dissociated and much of it settles on the PNS. Heating due to accretion onto the PNS drives the emission of neutrinos of all three flavors ($\nu_e$, $\nu_\mu$, $\nu_\tau$) and their anti-particles ($\bar{\nu}_e$, $\bar{\nu}_\mu$, $\bar{\nu}_\tau$). Below the shock, but above the PNS, the absorption of $\nu_e$ and $\bar{\nu}_e$ by the free nucleons results in a 'gain region' of net heating. In spherically symmetric (1D) simulations, fluid elements advect through the gain region before they can be heated sufficiently to reverse their direction and drive an explosion, thus 1D simulations of Fe-core collapse invariably end in the accretion of the entire star, a situation that is not matched by observations of CCSNe.

Neutrino heating may be aided by fluid instabilities (e.g., convection) in the PNS [1–5], which may boost the luminosity of the central neutrino source. Convection directly beneath the shock serves to markedly alter the state of the matter undergoing reheating via neutrino energy deposition [5–10] relative to the spherically symmetric case. This inherently multidimensional effect allows simultaneous downflows that fuel the neutrino luminosities by accretion and upflows that bring energy to the shock. A multidimensional instability of the shock wave itself, the *Standing Accretion Shock Instability* (SASI; [11]), also fundamentally changes the structure of the gain region in multidimensional simulations [11–14]. At the center of the configuration, the PNS is an extremely dense compact object, and its gravitational field is not well described by Newtonian gravity. Rather, general relativity (GR) is required to adequately describe the strong gravity inherent in the event. All of these phenomena serve to delineate and define the requisite level of physical fidelity that must be achieved by a CCSN simulation in order for it be predictive of either the explosion outcome or the produced observables. In short, multidimensional hydrodynamics coupled to sophisticated neutrino transport must be used along with a careful description of the nuclear reactions in the event. All of this, ultimately, must also be done in the context of general relativistic gravity.

Recent progress to uncover the details of the CCSN explosion mechanism has been impressive. 2D modeling has matured rapidly as more simulations have been performed by different groups with the requisite physics [15–22]. The focus now turns to quantitative differences that must be understood (note that some quantitative differences should be expected given the use of independent codes based on different numerical methods). Convergence of the simulation outcomes across groups must occur before we can claim to have gained solid insight into the fundamentals of the explosion mechanism. Here we describe some of the details of and results obtained with our own code to attack this problem in multidimensions: the Chimera code. We highlight the effects on nucleosynthetic signatures of performing self-consistent CCSN simulations in 2 and 3 dimensions with Chimera, including a possible mechanism to producing $^{48}$Ca made possible only through this combination of sufficient physical inputs and dimensionality.

## THE Chimera CODE

The name Chimera originates in its combination of three, separate, mature codes. The primary code modules evolve the stellar fluid dynamics (MVH3), the "ray-by-ray" neutrino transport (MGFLD-TRANS), and the thermonuclear kinetics (XNet). These three "heads" are augmented by a sophisticated equation of state for nuclear matter. Hydrodynamics are evolved using a dimensionally split, piecewise parabolic method (PPM) — a version of the publicly available astrophysics PPMLR hydrodynamics code VH1. Self-gravity is computed via multipole expansion in spherical harmonics. Spherical symmetric corrections to gravity for GR replace the non-GR (Newtonian) monopole ($\ell = 0$) term.

In the lower density regions outside the Fe-core, physical conditions require the use of a nuclear network to evolve the time-dependent abundances of nuclei. The nuclear network incorporated into Chimera is the publicly available nuclear network code XNet. XNet solves, for each non-equilibrium zone, a coupled system of non-linear ODEs (one for each nuclear species) for the time evolution of the nuclear abundances. Where the nuclear time step is smaller than the hydrodynamic step, XNet will compute multiple substeps automatically to prevent the short reaction timescales in a few zones from severely restricting the global simulation time step. Most Chimera simulations have used a 14-species $\alpha$-network ($^4$He,$^{12}$C–$^{60}$Zn). We have recently installed a more extensive network of 160 isotopes for elements through germanium [23] in the code. This improvement depends on pervasive threading of the network calculations to achieve tractable runtimes (i.e. not too much greater than the smaller $\alpha$-network ). We also typically use at least 100,000 Lagrangian tracer particles in 3D as data samplers for post-processing nucleosynthesis with a 4000+ isotope network in XNet and other analyses.

Transport of neutrinos is computed as multi-(energy)-group angular moments of the neutrino distribution function in a diffusive approximation which is flux-limited to prevent aphysical (i.e. superluminal) propagation of neutrinos in semi-transparent and transparent regions (multi-group flux-limited diffusion, or MGFLD). The MGFLD equations – including local couplings between all energy groups (via scattering), neutrinos and anti-neutrinos (via pair emission processes), and to the local matter – are solved implicitly along each radial 'ray' using the ray-by-ray approximation. The neutrino–matter interactions are a modern set that include scattering on electrons and free nucleons with energy exchange, emission and absorption on free nucleons and an ensemble of nuclei in NSE, and neutrino–anti-neutrino pair emission from nucleon-nucleon bremsstrahlung and $e^+e^-$-annihilation.

The spherical coordinates used in Chimera are natural for the CCSN problem given the centrally concentrated PNS and our use of the ray-by-ray approximation for neutrino transport. Using spherical coordinates allows better resolution of the radial structure of the PNS and helps limit error in the gravitational binding energy, which is the

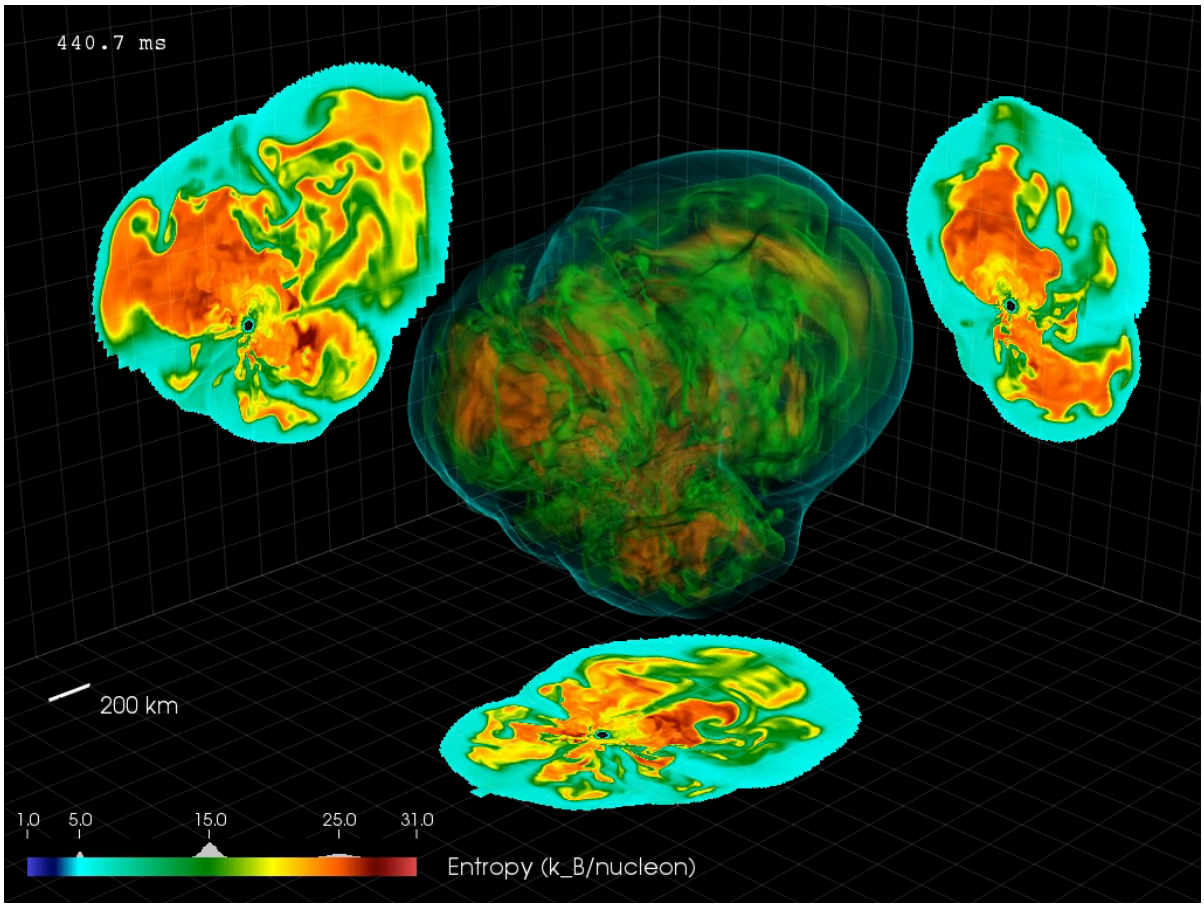


**FIGURE 1.** Entropy from a 3D CHIMERA simulation at 440 ms post-bounce. Shown is a volume rendering of the entropy below the shock, with slices through the three primary axes projected on the three surrounding planes. The grid marks are at 200 km (as indicated in the lower left).

ultimate energy source of the explosions. Orienting the primary computational domains along the radial direction results in similar conditions on each process for the most expensive computational elements (transport and nuclear burning) and natural load balancing of the computational work. Spherical coordinates come at the price of restricted lateral zone sizes (and time steps) from coordinate convergence at the center and the pole. The center in CHIMERA (and similar codes) is treated in spherical approximation, which suppresses non-radial motions in the inner part (i.e., the inner few km) of the PNS and relieves the simulation of the time step restrictions from the non-radial zone widths inside the spherical region. The convergence of the grid at the poles ($\theta = 0, \pi$) is the other limiting factor (the time step restricting length for the zone closest to the pole is $\Delta\ell = R\,\Delta\phi\,\sin\theta_c$). Other remedies have been brought to bear here, including Yin-Yang grids [24] and reduced $\phi$ resolution when approaching the pole (as was done in [19]).

## NUCLEOSYNTHESIS IN CCSNE AND THE EFFECT OF MULTIDIMENSIONS

Large overabundances of elements in the periodic table spanning from oxygen through nickel are observed in CCSNe and their remnants. Observations of nuclear abundances allow nucleosynthesis calculations to place powerful constraints on conditions deep in the interior of CCSNe and their progenitors, places hidden from direct observation. Unfortunately, until recently, the frequent failure of self-consistent models to produce explosions has resulted in the reliance of CCSN nucleosynthesis modeling on parameterized models, which replace the inner workings of the SN with a kinetic energy *piston* [see, e.g., 25–28] or a thermal energy *bomb* [see, e.g. 29–31]. In such bomb or piston

simulations, the explosion's energy, its delay time, and the *mass cut*, which separates the ejecta from matter destined to become part of the neutron star, are externally supplied parameters. The bomb and piston methods are largely comparable, with the largest differences coming in the inner regions of the ejecta [32]. However, it is the nucleosynthesis in this inner region that can be strongly affected by the details of the explosion mechanism [33]. In the case of the neutrino reheating mechanism, chief among these details are interaction with the tremendous flux of neutrinos and the temporal delay in achieving the explosion. In the innermost regions of the ejecta, the passage of the shock heats matter to temperatures where nuclear statistical equilibrium (NSE) is dominated by free nucleons and $\alpha$ particles [see, e.g., 34, 35]. As a result, much of the iron-peak species synthesized in CCSN result from *$\alpha$-rich freezeout* [36]. As matter expands outward, it cools, allowing the light nuclei to recombine into iron, nickel, and neighboring nuclei. In the case of $\alpha$-rich freezeout, this recombination is incomplete, leaving a significant fraction of the matter still in the form of free nucleons and $\alpha$ particles. The detailed composition of this ejecta depends on its electron fraction, which is set in the inner regions of the ejecta by neutrino interactions.

One common property exhibited by all recent 1- and 2-D simulations utilizing spectral neutrino transport [see, e.g., 5, 37–40] is a decrease in the neutronization in the outer part of the neutrino heating region, due to neutrino interactions. This is a property that the parameterized bomb/piston nucleosynthesis models discussed above cannot replicate because they ignore neutrinos. The neutronization is important because GCE calculations and the relative neutron poverty of terrestrial iron and neighboring elements strongly limit the amount of neutronized material that may be ejected into the interstellar medium by CCSN [41]. Hoffman *et al.* [42] placed a limit of $10^{-4} M_{\odot}$ on the typical amount of neutron-rich ($Y_e < 0.47$) ejecta allowed from each CCSN. Past multi-D models of CCSN using *gray* (energy-integrated or -averaged — i.e., not spectral) neutrino transport that did produce explosions tended to greatly exceed this limit [see, e.g., 6, 8].

## THE ORIGIN OF $^{48}$Ca

The doubly magic nature of $^{48}$Ca is key to its relatively large cosmic abundance. Indeed, $^{48}$Ca is almost 50 times more abundant than the incrementally lighter, but stable, $^{46}$Ca. Nevertheless, the origin of this most neutron-rich stable isotope below the iron peak has been a puzzle for more than three decades [see, e.g., 35, 43, and references therein, for more details on the historical background]. As a relatively bound nucleus for its neutron-richness, $^{48}$Ca is abundantly produced by nuclear statistical equilibrium for electron fractions ($Y_e$) near the $Z/A = 20/48 = 0.42$ of $^{48}$Ca. However, in the presence of a significant population of $\alpha$-particles, $^{48}$Ca is quickly destroyed by a series of ($\alpha$,n) reactions leading to production of many heavier nuclei of $A \lesssim 90$. Meyer, Krishnan, and Clayton [43] found that significant production of $^{48}$Ca is directly correlated with the photon-to-nucleon ratio, $\phi \equiv 0.34 T_9^3/\rho_5 \lesssim 1$, in the neutrino-driven ejecta, where $T_9$ is the temperature in units of $10^9$ GK and $\rho_5$ is the density in units of $10^5$ g cm$^{-3}$. They exclude CCSNe as a production site due to high entropies ($\phi > 1$) in the innermost ejecta, on the basis of one-dimensional parameterized explosion models, and therefore conclude that rare ($\approx$2%) varieties of Type Ia supernovae characterized by carbon deflagration at very high densities ($\rho \gtrsim 5 \times 10^9$g cm$^{-3}$) must be the astrophysical site of the production of $^{48}$Ca and the other low-mass neutron-rich isotopes of Ti, Cr, and Fe [43–45].

However, multi-dimensional CCSN models broaden the range of thermodynamic conditions experienced by the ejecta. Harris *et al.* [46] find that entrainment of neutron-rich matter by accretion streams that strike the PNS obliquely can lead to the ejection of suitably neutron-rich material with low enough $\phi$ for significant production of $^{48}$Ca. Wanajo, Janka, and Müller [47] found that similar dredge up from the outer layers of the PNS by convective overturn during the early stages of the explosion leads to the ejection of suitably neutron-rich material during electron-capture supernovae (ECSN). On the basis of post-processing nucleosynthesis studies, Wanajo, Janka, and Müller [48] found that significant production of $^{48}$Ca was possible, however this production was limited by moderate entropies ($\phi \sim 1$). Recent studies [20, 49] have shown that the lowest mass iron core collapse supernovae are dynamically very similar to ECSN, due to the similar light envelope of the star. Thus these lowest mass CCSN are also candidates for production of $^{48}$Ca. Figure 2, from a CHIMERA simulation for a 9.6 solar mass first generation star, using a fully coupled 160 species nuclear network, illustrates this production of $^{48}$Ca. Note that the $^{48}$Ca, produced in low entropy, and hence $\alpha$-poor freezeout, is above (produced earlier in the explosion) than the products of $\alpha$-rich freezeout, here highlighted by abundance of $^{44}$Ti. This highlights the greater range of thermodynamic conditions experienced by the ejecta of CCSN that is revealed by examining the nucleosynthesis of multi-dimensional models that include the full neutrino-driven convective engine of these supernovae.

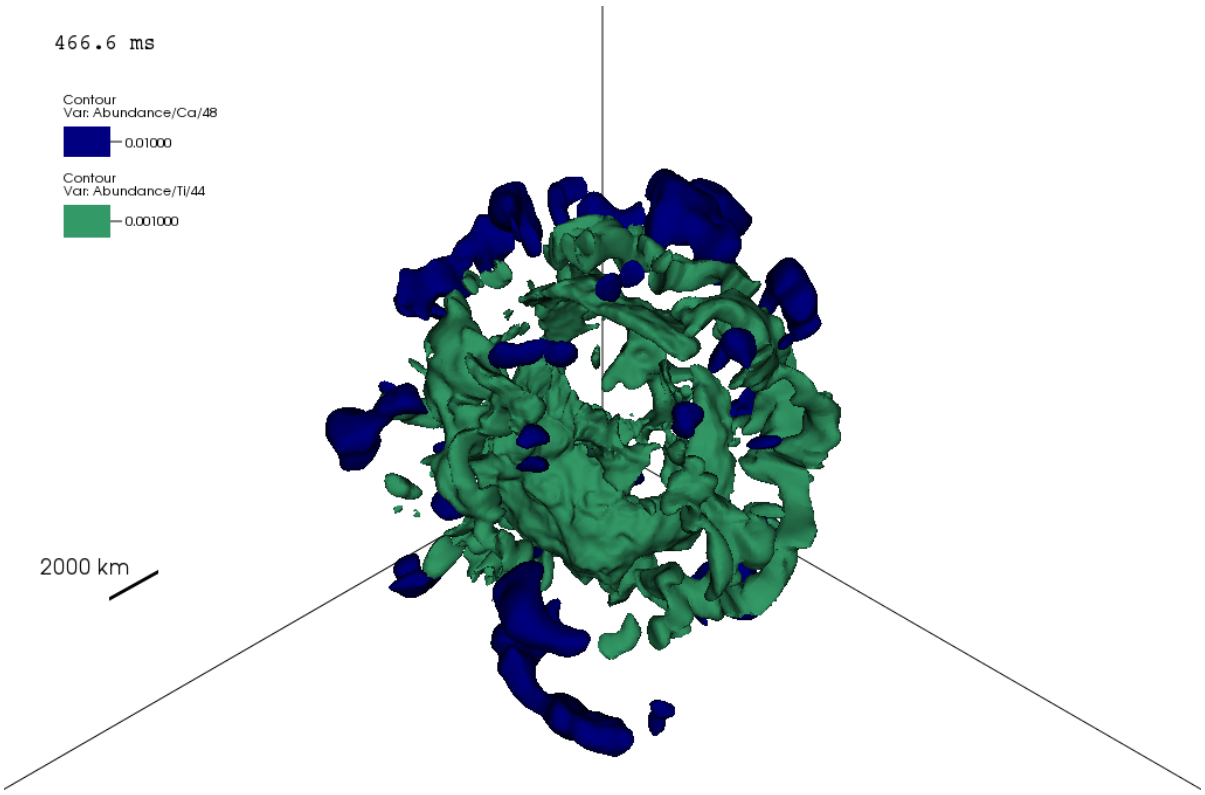


**FIGURE 2.** Abundance contours (of 0.01 and 0.001, respectively) of $^{44}$Ti and $^{48}$Ca at 466 ms postbounce from a 3D CHIMERA simulation of a light iron core. Note the distribution of $^{48}$Ca lies primarily outside the $^{44}$Ti.

## ACKNOWLEDGMENTS

This research used resources of the Oak Ridge Leadership Computing Facility at the Oak Ridge National Laboratory, which is supported by the Office of Science of the U.S. Department of Energy under Contract No. DE-AC05-00OR22725. This research was supported by the U.S. Department of Energy Offices of Nuclear Physics and Advanced Scientific Computing Research; the NASA Astrophysics Theory Program (grant NNH11AQ72I); and the National Science Foundation PetaApps Program (grants OCI-0749242, OCI-0749204, and OCI-0749248). This research is part of the Blue Waters sustained-petascale computing project, which is supported by the National Science Foundation (awards OCI-0725070 and ACI-1238993) and the state of Illinois. Blue Waters is a joint effort of the University of Illinois at Urbana-Champaign and its National Center for Supercomputing Applications. This work is also part of the "Core-collapse Supernovae Through Cosmic Time" Petascale Computational Resource (PRAC) allocation support by the National Science Foundation (award ACI-144005).

## REFERENCES

[1] L. Smarr, J. R. Wilson, R. T. Barton, and R. L. Bowers, ApJ **246**, 515–525 (1981).
[2] J. R. Wilson and R. W. Mayle, Phys. Rep. **227**, 97–111 (1993).
[3] J. A. Miralles, J. A. Pons, and V. A. Urpin, ApJ **574**, 356–363 (2002).
[4] S. W. Bruenn, E. A. Raley, and A. Mezzacappa, (2004), arXiv:astro-ph/0404099 [astro-ph] .
[5] R. Buras, M. Rampp, H.-T. Janka, and K. Kifonidis, A&A **447**, 1049–1092 (2006).
[6] M. Herant, W. Benz, W. R. Hix, C. L. Fryer, and S. A. Colgate, ApJ **435**, 339–361 (1994).

[7] A. Burrows, J. Hayes, and B. A. Fryxell, ApJ **450**, 830–850 (1995).
[8] H.-T. Janka and E. Müller, A&A **306**, 167–198 (1996).
[9] C. L. Fryer and M. S. Warren, ApJ **601**, 391–404 (2004).
[10] S. W. Bruenn, C. J. Dirk, A. Mezzacappa, J. C. Hayes, J. M. Blondin, W. R. Hix, and O. E. B. Messer, J. Phys.: Conf. Ser. **46**, 393–402 (2006).
[11] J. Blondin, A. Mezzacappa, and C. DeMarino, ApJ **584**, 971–980 (2003).
[12] H.-T. Janka, R. Buras, F. S. Kitaura Joyanes, A. Marek, M. Rampp, and L. Scheck, Nucl. Phys. A **758**, 19–26 (2005).
[13] A. Burrows, E. Livne, L. Dessart, C. D. Ott, and J. Murphy, ApJ **640**, 878–890 (2006).
[14] N. Ohnishi, K. Kotake, and S. Yamada, ApJ **641**, 1018–1028 (2006).
[15] B. Müller, H.-T. Janka, and A. Marek, ApJ **756**, p. 84 (2012).
[16] B. Müller, H.-T. Janka, and A. Heger, ApJ **761**, p. 72 (2012).
[17] S. W. Bruenn, A. Mezzacappa, W. R. Hix, E. J. Lentz, O. E. B. Messer, E. J. Lingerfelt, J. M. Blondin, E. Endeve, P. Marronetti, and K. N. Yakunin, ApJ **767**, p. L6 (2013).
[18] S. W. Bruenn, E. J. Lentz, W. R. Hix, A. Mezzacappa, J. A. Harris, O. E. B. Messer, E. Endeve, J. M. Blondin, M. A. Chertkow, E. J. Lingerfelt, P. Marronetti, and K. N. Yakunin, ApJ **818**, p. 123 (2016).
[19] E. J. Lentz, S. W. Bruenn, W. R. Hix, A. Mezzacappa, O. E. B. Messer, E. Endeve, J. M. Blondin, J. A. Harris, P. Marronetti, and K. N. Yakunin, ApJ **807**, p. L31 (2015).
[20] T. Melson, H.-T. Janka, and A. Marek, ApJ **801**, p. L24 (2015).
[21] T. Melson, H.-T. Janka, R. Bollig, F. Hanke, A. Marek, and B. Müller, ApJ **808**, p. L42 (2015).
[22] A. Burrows, D. Vartanyan, J. C. Dolence, M. A. Skinner, and D. Radice, ApJ p. submitted (2017), arXiv:1611.05859 [astro-ph.SR] .
[23] M. A. Chertkow, O. E. B. Messer, W. R. Hix, K. Yakunin, P. Marronetti, S. W. Bruenn, E. J. Lentz, J. Blondin, and A. Mezzacappa, J. Phys.: Conf. Ser. **402**, p. 012025 (2012).
[24] A. Kageyama and T. Sato, Geochemistry, Geophysics, Geosystems **5**, p. Q09005 (2004).
[25] S. E. Woosley and T. A. Weaver, ApJS **101**, 181–235 (1995).
[26] T. Rauscher, A. Heger, R. D. Hoffman, and S. E. Woosley, ApJ **576**, 323–348 (2002).
[27] M. Limongi and A. Chieffi, ApJ **592**, 404–433 (2003).
[28] S. E. Woosley and A. Heger, Phys. Rep. **442**, 269–283 (2007).
[29] F.-K. Thielemann, K. Nomoto, and M. Hashimoto, ApJ **460**, 408–436 (1996).
[30] S. Nagataki, T. M. Shimizu, and K. Sato, ApJ **495**, p. 413 (1998).
[31] H. Umeda and K. Nomoto, ApJ **673**, 1014–1022 (2008).
[32] M. B. Aufderheide, E. Baron, and F. K. Thielemann, ApJ **370**, 630–642 (1991).
[33] C. Fryer, P. Young, M. E. Bennet, S. Diehl, F. Herwig, R. Hirschi, A. Hungerford, M. Pignatari, G. Magkotsios, G. Rockefeller, and F. X. Timmes, "Nucleosynthesis from supernovae as a function of explosion energy from NuGrid," in *Proceedings of Nuclei in the Cosmos X*, edited by H. Schatz, S. Austin, T. Beers, A. Brown, E. Brown, R. Cyburt, W. Lynch, and R. Zegers (SISSA Proceedings of Science, 2008) p. 101.
[34] F. E. Clifford and R. J. Tayler, Mem. RAS **69**, p. 21 (1965).
[35] D. Hartmann, S. E. Woosley, and M. F. El Eid, ApJ **297**, 837–845 (1985).
[36] S. E. Woosley, W. D. Arnett, and D. D. Clayton, ApJS **26**, 231–312 (1973).
[37] M. Liebendörfer, A. Mezzacappa, F.-K. Thielemann, O. E. B. Messer, W. R. Hix, and S. W. Bruenn, Phys. Rev. D **63**, p. 103004 (2001).
[38] M. Rampp and H.-T. Janka, A&A **396**, 361–392 (2002).
[39] A. Marek and H.-T. Janka, ApJ **694**, 664–696 (2009).
[40] S. W. Bruenn, A. Mezzacappa, W. R. Hix, J. M. Blondin, P. Marronetti, O. E. B. Messer, C. J. Dirk, and S. Yoshida, *Proceedings of SciDAC 2009*, J. Phys.: Conf. Ser. **180**, p. 012018 (2009).
[41] V. Trimble, A&AR **3**, 1–46 (1991).
[42] R. D. Hoffman, S. E. Woosley, G. M. Fuller, and B. S. Meyer, ApJ **460**, 478–488 (1996).
[43] B. S. Meyer, T. D. Krishnan, and D. D. Clayton, ApJ **462**, p. 825 (1996).
[44] S. E. Woosley, ApJ **476**, 801–810 (1997).
[45] S. E. Woosley, A. Heger, and T. A. Weaver, Rev. Mod. Phys. **74**, 1015–1071 (2002).
[46] J. A. Harris, W. R. Hix, M. A. Chertkow, S. W. Bruenn, E. J. Lentz, O. E. B. Messer, A. Mezzacappa, J. M. Blondin, E. Endeve, E. J. Lingerfelt, P. Marronetti, and K. N. Yakunin, ApJ (in prep).
[47] S. Wanajo, H.-T. Janka, and B. Müller, ApJ **726**, p. L15 (2011).
[48] S. Wanajo, H.-T. Janka, and B. Müller, ApJ **767**, p. L26 (2013).
[49] E. J. Lentz, W. R. Hix, J. A. Harris, S. W. Bruenn, O. E. B. Messer, A. Mezzacappa, J. M. Blondin, and C. M. Mauney, ApJ (in prep).